Hindawi Publishing Corporation
Mathematical Problems in Engineering
Volume 2013, Article ID 593601, 9 pages
http://dx.doi.org/10.1155/2013/593601

Research Article

Numerical Simulation of Air Inlet Conditions Influence on the Establishment of MILD Combustion in Stagnation Point Reverse Flow Combustor

Xiao Liu and Hongtao Zheng

College of Power and Energy Engineering, Harbin Engineering University, Harbin, Heilongjiang 150001, China

Correspondence should be addressed to Xiao Liu; liuxiao_heu@163.com

Received 27 March 2013; Revised 24 April 2013; Accepted 24 April 2013

Academic Editor: Zhijun Zhang

This paper presents a numerical study of the nonpremixed stagnation point reverse flow (SPRF) combustor, especially focusing on the influence of air inlet conditions. Modified eddy dissipation concept (EDC) with a reduced mechanism was used to calculate the characteristic of MILD combustion. The results show that the modified EDC with DRM19 mechanism is suitable for the present simulations. Seven additional runs are conducted to find out that it is not necessary to include the influence of low oxygen despite its conduciveness to the establishment of MILD combustion in SPRF combustor. In addition, for the same mass rate of air inlet, it is difficult to reach MILD combustion mode by changing the velocity of the air inlet. The influence of air inlet momentum is also investigated by keeping the air inlet velocity constant and increasing the mass. Although the degree of recirculation (R_{eg}) is small, it can still achieve MILD combustion mode. Compared with the influence of air inlet velocity, it could be concluded that, rather than R_{eg}, the recirculation flow rate is the most important factor.

1. Introduction

With the world's increasing care for purifying and sustainability of environment, moderate or intense low-oxygen dilution combustion (MILD) [1] is becoming a credible candidate to simultaneously meet the mitigation of combustion-generated pollutants (NO_x) and greenhouse gases (CO_2) whilst meeting combustion efficiency needs. When the MILD combustion occurs, particularly firing gas and light oil, the entire furnace is bright and transparent and no flame is visible, so that it is often called "flameless combustion (FLOX) [2]" or "colorless combustion." This combustion is also named "high temperature air combustion" (HiTAC) [3] because the combustion air is usually preheated to beyond 1200 K for industrial regenerative combustor systems.

The German and Japanese researchers found at the beginnings of the 1990s that when preheating the air with regenerator to about 1600 K and injecting it approximately at 90 m/s, the visible flame disappeared and formed as the MILD combustion. Katsuki and Hasegawa [4] and J. Wünning and J. Wünning [2] reviewed advances in heat recirculating combustion in industrial furnaces and found that the recirculation of burned gases and preheating air with low oxygen concentration for hot coflow combustion. were shown to be indispensable factors in realizing MILD combustion with low nitric oxide emissions. Dally et al. [5] reported a jet in hot coflow (JHC) burner which consists of an insulated and cooled central fuel jet and an annulus with a secondary burner. The secondary burner provides hot combustion products which are mixed with air and nitrogen using two side inlets upstream of the annulus exit, to control the oxygen level in the mixture. The cold mixture of air and nitrogen also assists in the cooling of the secondary burner. Oldenhof et al. [6] reported on the Delft jet-in-hot coflow (DJHC) burner which is based on that of Dally to study ignition kernels appearance. It is generally believed that the MILD combustion has to be achieved by preheating the air above the ignition point.

The air preheating requirements of the high temperature air combustion system limits the application of the MILD combustion technology. Because the reversed flow combustion configuration can avoid this procedure, more

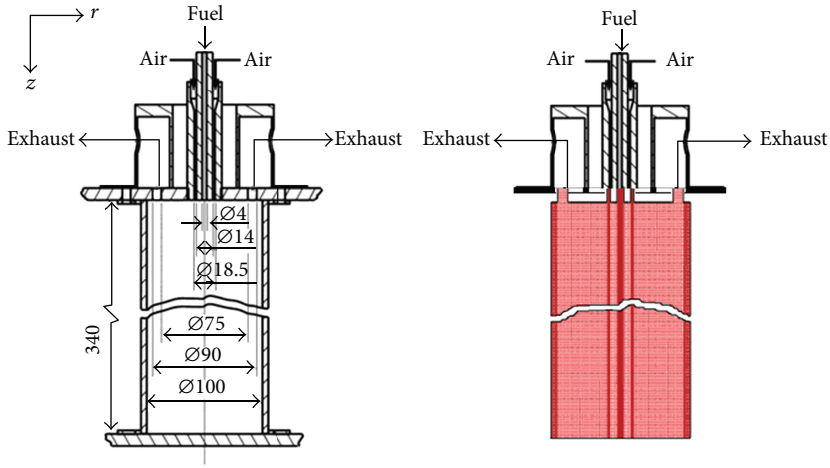

Figure 1: The schematic of the combustor and mesh of computational domain.

and more attention was focused here. Yang and Blasiak [7] showed that flameless oxidation can only be reached if the inlet velocities of the reactants are high enough to establish recirculation zones in the reversed flow combustion chamber. Unfortunately, high velocity of air inlet will lead to combustion instabilities, insufficient residence time, and high CO emission.

These issues may be overcome by a combustor design where both the burner and the exhaust port were mounted at the same end of the combustion chamber. Bobba et al. [8] developed a premixed Stagnation Point Reverse Flow (SPRF) combustor, and various optical diagnostic techniques were employed to elucidate the combustion processes in this novel combustor. The results showed that the SPRF combustor achieved internal exhaust gas recirculation and efficient mixing, which eliminated local peaks in temperature. Szegö et al. [9, 10] described the performance and stability characteristics of a parallel jet MILD combustion burner, the influence of equivalence ratio, combustion air temperature and heat extraction on performance were presented. Castela et al. [10] examined the combustion regimes occurring in a small-scale laboratory cylindrical combustor, in which the inlet and outlet were in the same side. The combustion regime developed from conventional lean combustion to flameless combustion by changing excess air coefficients (λ) and detailed in-combustor measurements of temperature and O_2, CO_2, CO, unburned hydrocarbons, and NO_x concentrations were reported.

On the other hand, many of these experimental studies have been complemented with Computational Fluid Dynamics (CFD) simulations. Kim et al. [11] investigated a global reaction mechanism for natural gas combustion to predict the observed nitrogen oxide and carbon monoxide levels in MILD combustion mode and concluded that the EDC turbulence-chemistry interaction model is suitable for the calculation of MILD combustion processes. Christo and Dally [12] found the EDC model with a detailed kinetic scheme, offering a practical and reasonably accurate tool for predicting the flow and flame characteristics of JHC configurations. Parente et al. [13] found a simple NO formation mechanism based on the thermal and prompt routes which is found to provide NO emissions in relatively good agreement with experimental observations only when applied on temperature fields obtained with the EDC model and detailed chemistry. Galletti et al. [14] also found by CFD simulations that to save the computation time for engineering applications the 3D simulation of the MILD combustion should be simplified to the 2D case. They found quite small differences between the 2D and 3D calculations.

The present study is aimed at accurately capturing the characteristics of MILD combustion in this reversed flow small-scale combustor, using the modified Eddy Dissipation Concept (EDC) model with detailed mechanism. According to the test conditions of M. Castela [10], there are two variables from conventional lean combustion to flameless combustion: the total content of oxygen and the momentum (mass and velocity) of the air inlet; therefore, the main objective of the simulations is to investigate and explain the air inlet conditions impact on the establishment of MILD combustion.

2. Computation Details

2.1. Furnace Configuration and Fuel. Figure 1 shows the schematic of the combustor used in this study. The combustion chamber is a quartz-glass cylinder with an inner diameter of 100 mm and a length of 340 mm. During the tests, the quartz cylinder was insulated with a 30 mm thick ceramic fiber blanket. The burner and the exhaust port are mounted at the top end of the combustion chamber. The burner consists of a central orifice of 4 mm inner diameter, through which the fuel is supplied, surrounded by an annular orifice with 14 mm inner diameter and 18.5 mm outer diameter for the combustion air supply. The exhaust consists of an annular orifice, concentric with the burner, with 75 mm inner diameter and 90 mm outer diameter. A stainless steel plate is used to close the bottom end of the combustion chamber. This plate contains a moving hole with an inner diameter of 11 mm that allows for the introduction of probes. In this study, the natural gas (CH_4: 83.7%, C_2H_6: 7.6%, C_3H_8: 1.9%, N_2: 5.4%,

and other components with minor concentrations) was used as fuel.

2.2. Computational Conditions and Models. The governing equations are solved using CFD package ANSYS FLUENT 12.0. A two-dimensional mesh of the furnace was generated with the axial symmetry hypothesis to save the calculation cost; see also Figure 1. It is clear that the grids in the area of inlet and near the wall were refined; the optimal grid size was 22,563 cells after grid independent verification.

The SIMPLE method was used for velocity-pressure coupling. A second-order discretization scheme was used to solve all governing equations. Solution convergence was determined by two criteria. Standard wall functions were used for the velocity boundary conditions at the walls of the combustor. The wall temperature was set to 1300 K, based on experimental measurements, and the emissivity was set to 0.9. The first is ensuring that the residuals of the solved equations drop below specified thresholds set at 10^{-3} for all variables, while a residual of 10^{-6} was used for the energy equation. The second convergence criterion is ensuring that the value of a sensitive property (e.g., concentration of a radical species) at a critical spatial location has stabilized and is no longer changing with iterations.

2.2.1. Turbulence Model. Favre-averaged Navier-Stokes equations are solved by the standard k-ε turbulence model. It is a semiempirical model based on model transport equations for the turbulence kinetic energy (k) and its dissipation rate (ε) which has become the workhorse of practical engineering flow calculations in the time since it was proposed by Launder and Spalding [15].

2.2.2. Combustion Model. The oxidation reaction has been taken into account using the Eddy Dissipation Concept (EDC) combustion model. The EDC is a compromise of accuracy and computational cost and was successfully applied to different regimes of combustion and steam cracking using detailed reaction mechanisms. It considers the interaction between the turbulence and the reaction and assumes that the molecular mixing and the reaction take place in small turbulent structures, called small scales. The length fraction of the small scales is modeled as [16]

$$\gamma = C_\gamma \left(\frac{\upsilon\varepsilon}{k^2}\right)^{1/4}, \quad \text{with } C_\gamma = 2.1377. \tag{1}$$

The volume fraction of the small scales is calculated as γ^3. Species are assumed to react in the fine structures over a time scale:

$$\tau = C_\tau \left(\frac{\upsilon}{\varepsilon}\right)^{1/2}, \quad \text{with } C_\tau = 0.4082. \tag{2}$$

The mean source term in the conservation equation for the species i is modeled as

$$R_i = \frac{\rho\gamma^2}{\tau\left(1-\gamma^3\right)}\left(Y_i^* - Y_i\right). \tag{3}$$

The species transport equation (conservation equation) is written as

$$\frac{\partial}{\partial t}\left(\rho Y_i\right) + \nabla\cdot\left(\rho\vec{v}Y_i\right) = -\nabla\cdot J_i + R_i. \tag{4}$$

The variable Y_i^* is the species mass fraction reached from the current value of Y_i by the action of the applied chemical reaction mechanism over a time scale τ. So in the EDC model the mean chemical state evolves via a linear relaxation process, typical for mixing, towards a reacted state which would be reached by a nonlinear reaction process after a time scale τ.

Both these constants have been set based on several experiments [17], and for most of combustion simulation, EDC model with default parameters can well capture the features of combustion field. However, for specific combustion conditions, which can only partly agree with the experimental data, for example, the effect of changing parameters on the prediction of high-pressure gasification process has been investigated by Rehm et al. [18]; early ignition of Delft-Jet-in-Hot-Coflow (DJHC) flame can be avoided with modified EDC by changing small structure volume and residence time constants; more detailed description of MEDC can be found in [19]. In this paper, the delay of ignition can be found comparing with experimental data, so the opposite change of C_γ and C_τ is proposed to improve predictions.

The computation of the reaction rate source terms is accelerated with the In Situ Adaptive Tabulation (ISAT) algorithm [20] embodied in the solver. The default ISAT tolerance (10^{-3}) was used until a moderately converged solution was obtained, and a smaller tolerance (10^{-4}) was set thereafter.

2.2.3. Reaction Mechanism. The DRM19 chemical mechanism [21] was used in this work to describe the combustion of natural gas which is a subset of the GRI-Mech 1.2 full mechanism, with 19 species and 84 reactions, developed to obtain the smallest set of reactions needed to closely reproduce the main combustion characteristics predicted by the full mechanism. A two-step global chemical kinetic mechanism for CH_4 was also used as comparison. In addition, one-step mechanism for C_2H_6 and C_3H_8 was applied.

2.2.4. Radiation Model. The discrete ordinate radiation model [22] was used in this work, as it is applicable across a wide range of optical thicknesses. Considering that the optical thickness in MILD flames is not well known, the DO model seems an appropriate choice. The model solves the radiative transfer equation (RTE) for a finite number of discrete solid angles across the computational domain. It also incorporates the weighted sum of gray gas model (WSGGM), in which spatial variation in the total emissivity is computed as a function of gas composition and temperature. The WSGGM is a reasonable compromise between the oversimplified gray gas model and a complete model, which takes into account particular absorption bands.

3. Results and Discussion

Table 1 presents the three experimental conditions in detail; excess air coefficient and air inlet momentum (velocity) are

Table 1: Three experiment conditions.

Run (experiment)	λ	A_{air} (mm^2)	V_{air} (m/s)
1	1.5	114.8	66
2	2	114.8	88
3	2.4	114.8	108

For all conditions: atmospheric pressure; fuel thermal input = 8 kW, fuel inlet velocity = 17.7 m/s; air inlet temperature = 600 K; fuel inlet temperature = 300 K.

both increased from run 1 to run 3. Although the MILD combustion mode was achieved, the influence of air inlet conditions was not clear and definite. Unlike the traditional burner, MILD combustion can be achieved without preheating the air deeply in SPRF combustor.

This section presents the numerical results. At first, numerical predictions are validated against the measurements of MILD combustion mode (run 3); then the air inlet conditions influence on the establishment of MILD combustion is simulated and analysed.

3.1. Characteristic Parameters of Combustion

3.1.1. Temperature Uniformity. Temperature uniformity ratio R_{tu} is used to describe the gas temperature field uniformity inside the furnace. Many published works [7, 9, 23–25] in the literature stated that MILD technology gives much more uniform temperature field than traditional combustion. Furnace gas temperature uniformity ratio as defined below was used to describe the quality of temperature field in the furnace:

$$R_{tu} = \frac{T_{max} - \overline{T}}{\overline{T}}, \tag{5}$$

when $R_{tu} = 0$ and there is no gas temperature gradient inside the furnace.

3.1.2. Degree of Recirculation. The flow pattern in the burner confirms the mechanism that promotes the exhaust gases recirculation. The degree of recirculation can be evaluated with the recirculation factor, defined as

$$R_{eg} = \frac{m_{eg}}{m_a + m_f} = \frac{m_{down} - m_{out}}{m_a + m_f}, \tag{6}$$

where m_{eg} is the mass flux of the recirculated exhaust gas and then entrained while $m_a + m_f$ denotes the total mass flow rate of injecting reactants. For this reversed flow furnace, m_{eg} is equal to the downward mass flux m_{down} in cross section of recirculation center removing m_{out}. In addition, m_{down} is calculated by

$$m_{down} = \iint_A \rho v\,(x, y)\,dx\,dy. \tag{7}$$

3.2. Assessment of the Numerical Model. Prior to analysis, CFD simulations need to be validated against the experimental data of temperature and species mole fraction in MILD combustion mode (run 3). The predicted and measured temperature and CO_2 and O_2 mole fraction are displayed in Figure 2 with different chemical mechanism, two-step global mechanism, and the DRM19 mechanism for CH_4; in addition, a modified EDC with DRM19 mechanism is used.

Four sections along the axis are selected for comparison, namely, 70 mm, 150 mm, 204 mm, and 272 mm. It could be easily found that the results above have similar trend with two mechanisms. Significant discrepancies can be observed in the first three sections in terms of temperature and CO_2 while mole fraction of O_2 is in good agreement relatively. The experimental data of temperature and CO_2 is higher than that of prediction near the centerline at 70 mm and 150 mm, which suggests that natural gas is in the slow oxidation state after 70 mm by DRM19 mechanism prediction; the outcome by global mechanism is even worse because combustion does not take place before 150 mm. For the same reason, mole fraction of O_2 has the opposite trend. From the last section 272 mm, the distribution of DRM19 mechanism is more uniform than the global mechanism. Hence, taking the computing time and accuracy into account, the DRM19 mechanism is suitable for the present simulations.

The measured field almost has no obvious gradient all over the furnace; the tested combustion mode can well capture the features of MILD combustion except for the chemistry and temperature field in the fuel jet region, although the sophisticated chemical equilibrium model EDC with detailed chemical mechanism is used. The EDC model with default values of model constants appears to predict the occurrence of ignition too lately. A change of both of the two EDC model constants is found to lead to better agreement in the predictions of temperature profiles: the time scale constant is decreased from default value of $C_\tau = 0.4082$ to $C_\tau = 0.2$ and the volume fraction constant is increased from default value of $C_\gamma = 2.1377$ to $C_\gamma = 5$. It is clear that using modified EDC parameters substantially improves the results.

Figure 3 shows the distributions of temperature in the furnace from run 1 to run 3. Two distinct conditions are observed when the air flow rate is changed; run 1 is a conventional lean combustion regime with local high-temperature region and run 3 corresponds to the MILD combustion regime with almost homogeneous distribution of temperature. The characteristic parameters of three combustion modes are listed in Table 2, which are used to determine whether the MILD combustion is established.

Table 2: Characteristic parameters of combustion.

Run	Peak temperature	R_{tu}	R_{eg}
1	1870.6 K	8.03%	70.9%
2	1530.8 K	4.87%	82.7%
3	1426.9 K	3.65%	90.7%

3.3. Influence of Air Inlet Oxygen Content. It is well known [14] that the most important factor for the establishment of MILD combustion is the assurance of local oxygen concentration to be less than 5%–10% in conventional MILD combustion system. As is mentioned in Table 3, the influence

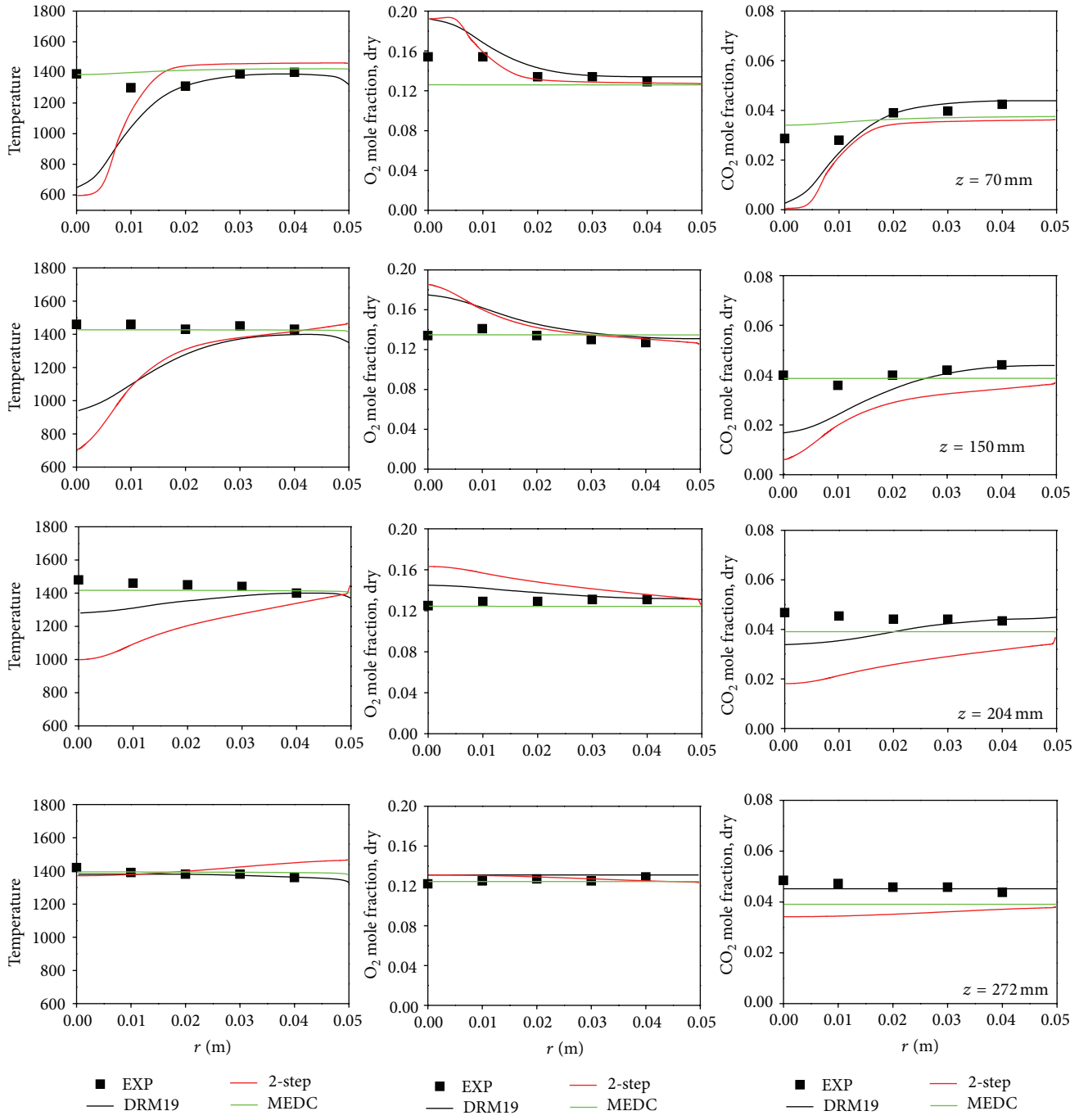

Figure 2: Comparison the predicted and measured temperature, CO_2 and O_2 mole fraction [10].

Table 3: CFD simulation conditions.

Run (CFD)	λ	A_{air} (mm^2)	V_{air} (m/s)
1	1.5	114.8	66
4	1	114.8	66
5	0.6	114.8	66

of oxygen content is calculated in runs 4 and 5 based on the conditions of run 1. The mole fraction of oxygen is cut down from 21% to 14% in run 4 and 8.7% (natural gas can completely react) in run 5 by diluting with nitrogen. The distribution of temperature in the furnace is shown in Figure 4. The ignition delay becomes longer, which means that the chemical reaction rate becomes slow, and it is the characteristic of MILD combustion. In addition, the peak temperature decreases and distributions of temperature become uniform with the drop of oxygen concentration, but the rate is very slight. Due to the dilution effect of high recirculated exhaust gas with fresh air, the content of O_2

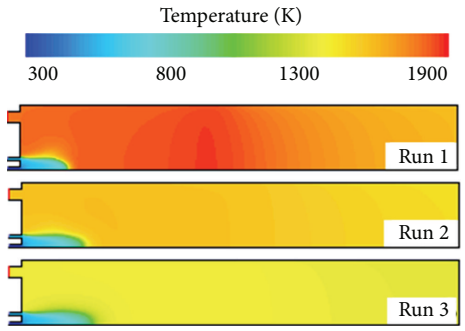

Figure 3: Distribution of temperature in the furnace from run 1 to run 3.

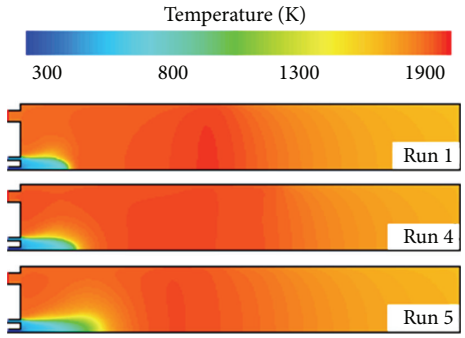

Figure 4: Distribution of temperature of runs 1, 4 and 5.

Table 4: CFD simulation conditions.

Run (CFD)	λ	A_{air} (mm^2)	V_{air} (m/s)
1	1.5	114.8	66
6*	1.5	88.3	86
7	1.5	71.7	106
8	1.5	42.9	176
9	1.5	153.1	66
10	1.5	187.8	66

*By keeping excess air coefficient constant with nitrogen dilution.

(almost less than 10%) meets the condition achieving MILD combustion.

Taking the complexity of the air dilution into account, the weak benefit of low oxygen content can be ignored. Therefore, there is no need to consider the influence of the oxygen, and standard air can be used in SPRF combustor.

3.4. Influence of Air Inlet Momentum. Consensus has been reached [26] that strong entrainment of high-temperature exhaust gases, which dilute fuel and air jets, is key technology of maintaining MILD combustion. However, from the velocity field of this combustor, the velocity is quite small near the bottom, where a quasi-stagnant region is present in SPRF combustor, so its mode of exhaust gas recirculation and dilution is different; thus the influence of air inlet momentum (mass and velocity) is simulated and the simulation conditions are listed in Table 4.

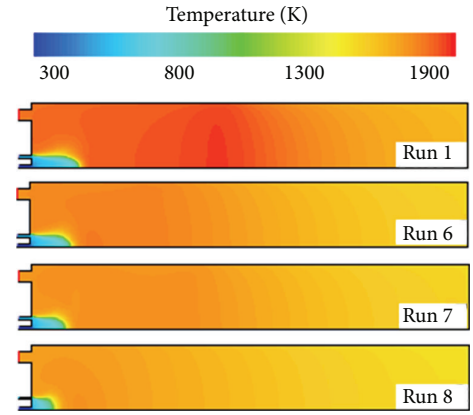

Figure 5: Distribution of temperature in the furnace of runs 1, 6, 7 and 8.

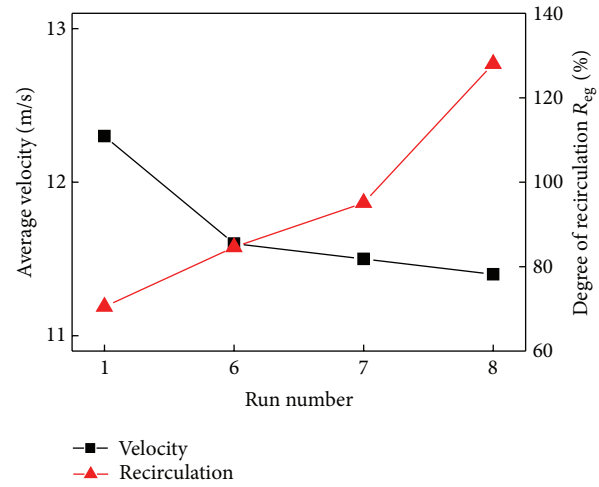

Figure 6: Trends of outlet average velocity and degree of recirculation.

3.4.1. Influence of Air Inlet Velocity. When the inlet mass flow rate of air remains constant, the area varies from 88.3 to 42.9 mm^2, which leads the air inlet momentum to almost three times as that of run 1. For these runs, although the peak temperature decreases, the traditional combustion with visible flames (high-temperature zone) is expected to occur as shown in Figure 5; the ignition delay time becomes shorter because of high turbulent intensity of inlet air, which will accelerate the mixing and reaction of fuel and air. In general, for the same mass flux of circular air jet, as A_{air} decreases, the air jet injection momentum increases and consequently the air and fuel jet entrainment with the recirculation of exhaust gas is enhanced. It is obviously beneficial for the establishment of MILD combustion. Although the velocity of run 7 is almost three times of run 1, the variation of temperature uniformity is getting smaller and smaller.

Figure 6 presents the trends of outlet average velocity and R_{eg}. It is evident that the outlet velocity decreases by a large amount from run 1 to run 6 due to the more strongly momentum of inlet air, so the exhaust gas remains

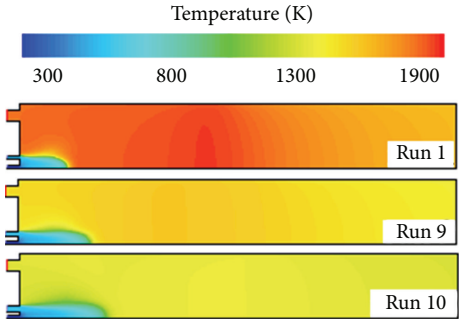

Figure 7: Distribution of temperature of runs 1, 9, and 10.

a longer time in the combustor; sufficient heat transfer with fresh air happened, which is beneficial for the establishment of MILD combustion, but the variation of outlet velocity decreases smaller and smaller from run 6 to run 8; the R_{eg} grows slowly from 85.1% to 128.8% and the rate of increase becomes more and more slowly. Many previous investigations were carried out to examine the influence of R_{eg} on MILD combustion [2, 27], and the results showed that in the MILD combustion zone, the internal recirculation rate (R_{eg}) was greater than 2.5. The importance of R_{eg} in the establishment of MILD combustion may be overemphasized because the flow development differs in various configuration furnaces.

After a comprehensive analysis, it is difficult to achieve the MILD combustion mode for SPRF combustor by simply changing the velocity of the air inlet considering the critical flow rate and the system complexity of increasing the velocity.

3.4.2. Influence of Air Inlet Mass. Runs 9 and 10 are calculated to investigate the influence of air inlet mass based on run 1, where the air inlet velocity keeps constant and inlet area becomes large to increase the inlet momentum. Figure 7 presents the contour of temperature in run 1, run 9, and run 10. The distribution of temperature becomes homogeneous at a fast rate, the peak temperature decreases from 1870.6 K to 1583.2 K and finally 1406.7 K, and the reaction rate of CH_4 decreases from 0.0717 kg/m^3·s to 0.0617 kg/m^3·s and finally 0.0537 kg/m^3·s, respectively. By comparison, the temperature uniformity is 3.68%, which is closer to that of the MILD combustion.

As presented in Figure 8, with the increase of the mass, R_{eg} first increases a little and then decreased. This is primarily because of the fact that the denominator in R_{eg} calculation formula $m_a + m_f$ grows faster than the rate of recirculation flow. The R_{eg} is only 66.8% in run 10, and it does not match the previous conclusion [2, 27] where the internal recirculation rate (R_{eg}) must be greater than 2.5. But the recirculation flow rate increases from 0.0032 to 0.005 kg/s, and the exhaust gas is sufficient to preheat and dilute the inlet air and it can still achieve to MILD combustion mode MILD combustion mode.

Figure 9 shows the fuel axial velocity in runs 1, 9, and 10. It can be seen that the fuel accelerates with the increase of air inlet mass, which means that the entrainment of the surrounding oxidant is enhanced due to the higher air inlet

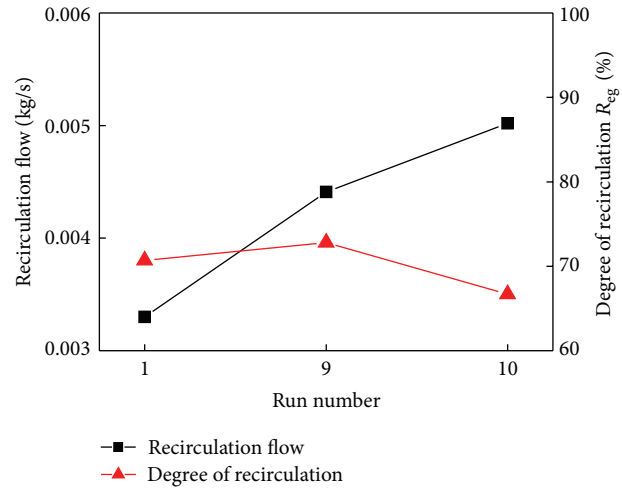

Figure 8: Trends of recirculation flow and degree of recirculation.

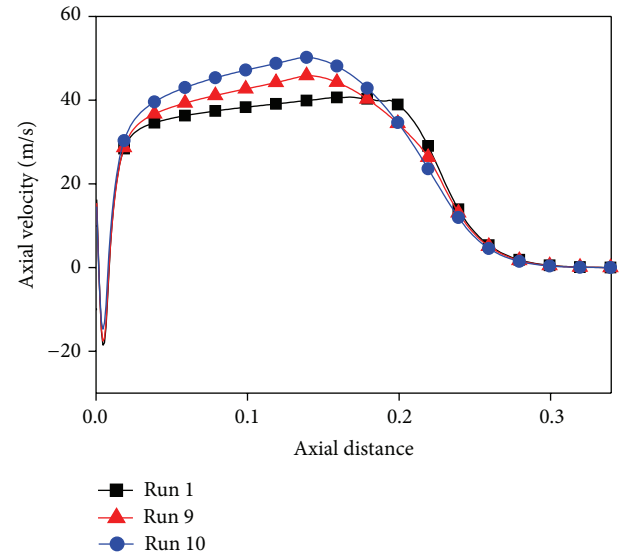

Figure 9: Fuel axial velocity along axis of runs 1, 9, and 10.

momentum. It provides some explanations as to why the MILD combustion can be established by increasing the mass of inlet air and without preheating the air for this configuration combustor according to the simulation. Compared with the influence of air inlet velocity, the recirculation flow is the most important factor, rather than R_{eg}. When reactants are preheated by exhaust gas, the mixture density decreases while their viscosity increases; it boosts the jet shear force and simultaneously increases the small-scale mixing and local scalar dissipation rate, thus hampering the formation of the flame front (local high temperature). Distributing the heat release to a larger volume leads to a nearly uniform temperature distribution with reduced peak temperatures. On the other hand, the high momentum gained by increasing air inlet mass strengthens exhaust recirculation and the influence of dilution on low oxygen concentration, which is also beneficial to the MILD combustion discussed previously.

4. Conclusions

A numerical study has been conducted to investigate the influence of air inlet conditions on the establishment of MILD combustion mode in an 8 kW nonpremixed Stagnation Point Reverse Flow (SPRF) combustor. The simulations are carried out by standard k-ε turbulence model and modified EDC combustion model with detailed mechanism DRM19; the combustion regime in the present combustor develops from conventional lean combustion to MILD combustion. The main conclusions are summarized as follows.

(1) Compared with experimental data, the modified EDC combustion model with DRM19 mechanism can well capture the features of MILD combustion when computing time and accuracy are taken into account.

(2) Based on the predicted data, reducing the oxygen content of air inlet is a little conducive to the establishment of MILD combustion, but the benefit of low oxygen content can be ignored due to the dilution effect of high recirculated exhaust gas with fresh air when the complexity of the air dilution is taken into account and standard air can be used in this SPRF combustor.

(3) For the same mass rate of air inlet, it is difficult to reach MILD combustion mode by simply changing the velocity of the air inlet. For the same inlet velocity, although R_{eg} is small (its trend first went up and then dropped), it can still achieve MILD combustion mode. Compared with the influence of air inlet velocity, it could be concluded that, rather than R_{eg}, the recirculation flow is the most important factor in SPRF combustor.

Nomenclature

k: Turbulent kinetic energy ($m^2 \cdot s^{-2}$)
Y_i^*: Fine-scale species mass fraction
Y_i: Local mass fraction of each species
S_i: Source term for the rate of creation species i
R_i: Net rate of production of species i
J_i: Diffusion flux of species i
C_γ: Volume fraction constant equal to 2.1377
C_τ: A time scale constant equal to 0.4082
R_{tu}: Temperature uniformity ratio
R_{eg}: Degree of recirculation
m_f: Mass flux of fuel inlet ($kg \cdot s^{-1}$)
m_{out}: Mass flux of flow out ($kg \cdot s^{-1}$)
m_a: Mass flux of air inlet ($kg \cdot s^{-1}$)
m_{down}: Downward mass flux ($kg \cdot s^{-1}$)
m_{eg}: Mass flux of the recirculated exhaust gas ($kg \cdot s^{-1}$)
$\overline{T}$: Average temperature (T)
T_{max}: Maximum temperature (T)
V_{air}: Velocity of air inlet ($m \cdot s^{-1}$)
A_{air}: Area of air inlet (mm^2).

Greek Symbols

ρ: Density of the mixture ($kg \cdot m^{-3}$)
λ: Excess air coefficients
ε: Kinetic energy dissipation rate ($m^2 \cdot s^{-3}$)
γ_λ: Mass fraction of fine structures
υ: Kinematic viscosity ($m^2 \cdot s^{-1}$)
τ^*: Mean residence time in fine structures (s).

References

[1] A. Cavaliere and M. De Joannon, "Mild combustion," *Progress in Energy and Combustion Science*, vol. 30, no. 4, pp. 329–366, 2004.

[2] J. Wünning and J. Wünning, "Flameless oxidation to reduce thermal NO-formation," *Progress in Energy and Combustion Science*, vol. 23, pp. 81–94, 1997.

[3] H. Tsuji, A. Gupta, T. Hasegawa, M. Katsuki, K. Kishimoto, and M. Morita, *High Temperature Air Combustion: From Energy Conservation to Pollution Reduction*, CRC Press, 2003.

[4] M. Katsuki and T. Hasegawa, "The science and technology of combustion in highly preheated air," *Proceedings of the Combustion Institute*, vol. 27, no. 2, pp. 3135–3146, 1998.

[5] B. B. Dally, A. N. Karpetis, and R. S. Barlow, "Structure of turbulent non-premixed jet flames in a diluted hot coflow," *Proceedings of the Combustion Institute*, vol. 29, no. 1, pp. 1147–1154, 2002.

[6] E. Oldenhof, M. J. Tummers, E. H. van Veen, and D. J. E. M. Roekaerts, "Ignition kernel formation and lift-off behaviour of jet-in-hot-coflow flames," *Combustion and Flame*, vol. 157, no. 6, pp. 1167–1178, 2010.

[7] W. Yang and W. Blasiak, "Flame entrainments induced by a turbulent reacting jet using high-temperature and oxygen-deficient oxidizers," *Energy and Fuels*, vol. 19, no. 4, pp. 1473–1483, 2005.

[8] M. K. Bobba, P. Gopalakrishnan, J. M. Seitzman, and B. T. Zinn, "Characteristics of combustion processes in a stagnation point reverse flow combustor," in *Proceedings of the ASME Turbo Expo 2006: Power for Land, Sea and Air*, GT2006-91217, pp. 867–875, Barcelona, Spain, May 2006.

[9] G. G. Szegö, *Experimental and numerical investigation of a parallel jet MILD combustion burner system in a laboratory-scale furnace [Ph.D. thesis]*, The University of Adelaide, Adelaide, Australia, 2010.

[10] M. Castela, A. S. Verissimo, A. M. A. Rocha, and M. Costa, "Experimental study of the combustion regimes occurring in a laboratory combustor," *Combustion Science and Technology*, vol. 184, pp. 243–258, 2012.

[11] J. P. Kim, U. Schnell, and G. Scheffknecht, "Comparison of different global reaction mechanisms for MILD combustion of natural gas," *Combustion Science and Technology*, vol. 180, no. 4, pp. 565–592, 2008.

[12] F. C. Christo and B. B. Dally, "Modeling turbulent reacting jets issuing into a hot and diluted coflow," *Combustion and Flame*, vol. 142, no. 1-2, pp. 117–129, 2005.

[13] A. Parente, C. Galletti, and L. Tognotti, "Effect of the combustion model and kinetic mechanism on the MILD combustion in an industrial burner fed with hydrogen enriched fuels," *International Journal of Hydrogen Energy*, vol. 33, no. 24, pp. 7553–7564, 2008.

[14] C. Galletti, A. Parente, and L. Tognotti, "Numerical and experimental investigation of a mild combustion burner," *Combustion and Flame*, vol. 151, no. 4, pp. 649–664, 2007.

[15] B. E. Launder and D. B. Spalding, *Lectures in Mathematical Models of Turbulence*, Academic Press, London, UK, 1972.

[16] I. R. Gran and B. F. Magnussen, "A numerical study of a bluff-body stabilized diffusion flame. Part 2: influence of combustion modeling and finite-rate chemistry," *Combustion Science and Technology*, vol. 119, no. 1–6, pp. 191–217, 1996.

[17] I. S. Ertesvåg and B. F. Magnussen, "The Eddy dissipation turbulence energy cascade model," *Combustion Science and Technology*, vol. 159, no. 1–6, pp. 213–235, 2000.

[18] M. Rehm, P. Seifert, and B. Meyer, "Theoretical and numerical investigation on the EDC-model for turbulence-chemistry interaction at gasification conditions," *Computers and Chemical Engineering*, vol. 33, no. 2, pp. 402–407, 2009.

[19] A. De, E. Oldenhof, P. Sathiah, and D. Roekaerts, "Numerical simulation of Delft-Jet-in-Hot-Coflow (DJHC) flames using the eddy dissipation concept model for turbulence-chemistry interaction," *Flow, Turbulence and Combustion*, vol. 87, no. 4, pp. 537–567, 2011.

[20] S. B. Pope, "Computationally efficient implementation of combustion chemistry using in situ adaptive tabulation," *Combustion Theory and Modelling*, vol. 1, no. 1, pp. 41–63, 1997.

[21] A. Kazakov and M. Frenklach, http://www.me.berkeley.edu/drm/.

[22] E. H. Chui and G. D. Raithby, "Computation of radiant heat transfer on a nonorthogonal mesh using the finite-volume method," *Numerical Heat Transfer*, vol. 23, no. 3, pp. 269–288, 1993.

[23] B. Danon, E.-S. Cho, W. De Jong, and D. J. E. M. Roekaerts, "Numerical investigation of burner positioning effects in a multi-burner flameless combustion furnace," *Applied Thermal Engineering*, vol. 31, no. 17-18, pp. 3885–3896, 2011.

[24] A. S. Veríssimo, A. M. A. Rocha, and M. Costa, "Operational, combustion, and emission characteristics of a small-scale combustor," *Energy and Fuels*, vol. 25, no. 6, pp. 2469–2480, 2011.

[25] A. S. Veríssimo, A. M. A. Rocha, and M. Costa, "Importance of the inlet air velocity on the establishment of flameless combustion in a laboratory combustor," *Experimental Thermal and Fluid Science*, vol. 44, pp. 75–81, 2013.

[26] E. Abtahizadeh, J. van Oijen, and P. De Goey, "Numerical study of mild combustion with entrainment of burned gas into oxidizer and/or fuel streams," *Combustion and Flame*, vol. 159, no. 6, pp. 2155–2165, 2012.

[27] A. Effuggi, D. Gelosa, M. Derudi, and R. Rota, "Mild combustion of methane-derived fuel mixtures: natural gas and biogas," *Combustion Science and Technology*, vol. 180, no. 3, pp. 481–493, 2008.